Journal of Hazardous Materials 164 (2009) 473–482

Contents lists available at ScienceDirect

Journal of Hazardous Materials

journal homepage: www.elsevier.com/locate/jhazmat

Adsorption isotherms, kinetics, thermodynamics and desorption studies of 2,4,6-trichlorophenol on oil palm empty fruit bunch-based activated carbon

I.A.W. Tan, A.L. Ahmad, B.H. Hameed*

School of Chemical Engineering, Universiti Sains Malaysia, Engineering Campus, 14300 Nibong Tebal, Penang, Malaysia

ARTICLE INFO

Article history:
Received 16 May 2008
Received in revised form 8 August 2008
Accepted 11 August 2008
Available online 19 August 2008

Keywords:
Oil palm empty fruit bunch activated carbon
2,4,6-Trichlorophenol
Isotherm
Kinetics
Desorption

ABSTRACT

The adsorption characteristics of 2,4,6-trichlorophenol (TCP) on activated carbon prepared from oil palm empty fruit bunch (EFB) were evaluated. The effects of TCP initial concentration, agitation time, solution pH and temperature on TCP adsorption were investigated. TCP adsorption uptake was found to increase with increase in initial concentration, agitation time and solution temperature whereas adsorption of TCP was more favourable at acidic pH. The adsorption equilibrium data were best represented by the Freundlich and Redlich–Peterson isotherms. The adsorption kinetics was found to follow the pseudo-second-order kinetic model. The mechanism of the adsorption process was determined from the intraparticle diffusion model. Boyd plot revealed that the adsorption of TCP on the activated carbon was mainly governed by particle diffusion. Thermodynamic parameters such as standard enthalpy (ΔH°), standard entropy (ΔS°), standard free energy (ΔG°) and activation energy were determined. The regeneration efficiency of the spent activated carbon was high, with TCP desorption of 99.6%.

1. Introduction

Cholorophenols are a group of chemicals in which chlorines (between one and five) have been added to phenol. The main pollution sources containing chlorophenols are the wastewaters from pesticide, paint, pharmaceutics, wood, paper and pulp industries as well as water disinfecting process [1]. Chlorophenols are weak acids which permeate human skin by in vitro and are readily absorbed by gastro-intestinal tract [2]. 2,4,6-Trichlorophenol (TCP) is a toxic, mutagenic and carcinogenic pollutant. It is found in the emissions from fossil fuel combustion, municipal waste incineration and chlorination of water containing phenol or certain aromatic acids with hypochlorite or during disinfection of water [3]. TCP has been also reported to cause adverse effects on human nervous system and respiratory problems such as chronic bronchitis, cough and altered pulmonary function [4]. The stable C—Cl bond and the position of chlorine atoms relative to the hydroxyl group are responsible for their toxicity and persistence in the biological environment [5]. Due to its high toxicity, carcinogenic properties, structural stabilization and persistence in the environment, the removal of TCP from the environment is crucial.

From the literature, various treatment methods have been applied to remove phenolic compounds from aqueous solutions, such as biological treatment using anaerobic granular sludge [1], catalytic wet oxidation [3], photochemical treatment [6], adsorption technology using activated clay [4], fuel oil fly ash [7] and activated carbons prepared from various precursors such as rattan sawdust, coconut shell and rice straw [8–10]. Other treatment technologies include air stripping, incineration, ion exchange and solvent extraction [4]. Adsorption on activated carbon is one of the most effective and widely used techniques in treating high strength and low volume of phenolic wastewaters [2]. Commercially available activated carbons like F300 granular activated carbons from Calgon Corp, Pittsburgh, PA are commonly used for the adsorption of chlorophenols [11]. However, the usage of activated carbon has been limited by its high cost due to the use of non-renewable and relatively expensive starting material such as coal, which is a major economic consideration [12]. This has prompted a growing research interest in the production of low cost activated carbons especially for application concerning wastewater treatment.

Recently, focus has been given on the preparation of activated carbons from agricultural by-products such as almond shell [13], bean pod [14], rice husk [15], cherry stone [16], date palm seed [17], sunflower seed hull [18], waste apricot [19], oil palm fibre [20], bamboo [21], plum kernel [22] and coconut husk [23,24]. Besides, not many studies have been reported in the literature on the adsorption of TCP using agricultural waste-based activated carbon. In practice, the feasibility of activated carbon adsorption process depends on many factors including the feasibility of regeneration and disposal of spent activated carbon. Therefore, the spent activated carbon

* Corresponding author. Fax: +60 4 594 1013.
E-mail address: chbassim@eng.usm.my (B.H. Hameed).

0304-3894/$ – see front matter © 2008 Elsevier B.V. All rights reserved.
doi:10.1016/j.jhazmat.2008.08.025

should have high regeneration efficiency for wider application of carbon adsorption process. Solvent regeneration in which carbon loss by attrition is negligible has been shown to be an attractive alternative. Hamdaoui et al. [25] in their study on regenerating granular activated carbon saturated with *p*-chlorophenol revealed that the desorption rate was enhanced by the addition of ethanol. Ethanol desorption technique was also reported to be suitable for regenerating activated carbons prepared from waste tires which showed high regeneration efficiencies for phenol and reactive dyes [26].

In the present investigation, oil palm empty fruit bunch-based activated carbon prepared under optimum conditions was evaluated for its potential to remove TCP from aqueous solutions. The equilibrium and kinetic data of the adsorption process were then analyzed to study the adsorption isotherms, kinetics, thermodynamics and mechanism of TCP on the prepared activated carbon. The feasibility of regenerating the spent activated carbon using ethanol desorption was then determined.

2. Materials and methods

2.1. Activated carbon preparation

The oil palm empty fruit bunch (EFB) used for preparation of activated carbon in this study was obtained from a local palm oil mill. The activated carbon preparation procedure was referred to our previous work [24] where the pre-treated EFB was loaded in a stainless steel vertical tubular reactor placed in a tube furnace and the carbonization of the precursor was carried out by ramping the temperature from room temperature to 700 °C with heating rate of 10 °C/min and hold for 2 h. Throughout the carbonization process, purified nitrogen (99.995%) was flown through at flow rate of 150 cm^3/min. The activated carbon was prepared using physiochemical activation method consisting of potassium hydroxide (KOH) treatment followed by carbon dioxide (CO_2) gasification by applying the optimum operating conditions which gave a high activated carbon yield and TCP uptake. The char produced from the carbonization process was mixed with KOH pallets with KOH:char impregnation ratio (IR) of 2.8:1. The dried mixture was then activated under the same condition as carbonization, but to a final temperature of 814 °C. Once the final temperature was reached, the nitrogen gas flow was switched to CO_2 and activation was held for 1.9 h. The activated product was then cooled to room temperature under nitrogen flow and then washed with hot deionized water and 0.1 M HCl until the pH of the washing solution reached 6–7.

2.2. 2,4,6-Trichlorophenol

2,4,6-Trichlorophenol supplied by Sigma–Aldrich (M) Sdn Bhd, Malaysia was used as the adsorbate in this study, and was not purified prior to use. TCP has a chemical formula of $C_6H_3Cl_3O$, with molecular weight of 197.46 g/mol. The chemical structure of TCP is shown in Appendix A. Deionized water supplied by USF ELGA water treatment system was used to prepare all the reagents and solutions.

2.3. Batch equilibrium studies

Batch equilibrium tests were carried out for adsorption of TCP on the activated carbon prepared. The effects of TCP initial concentration, agitation time, solution pH and temperature on the adsorption uptake were investigated. The sample solutions were withdrawn at equilibrium to determine the residual concentrations. The solutions were filtered using syringe filter prior to analysis in order to minimize interference of the carbon fines with the analysis. The concentrations of TCP in the supernatant solutions before and after adsorption were determined using a double beam UV–vis spectrophotometer (Shimadzu UV-1601, Japan) at its maximum wavelength of 296 nm. The TCP uptake at equilibrium, q_e (mg/g), was calculated by Eq. (1).

$$q_e = \frac{(C_0 - C_e)V}{W} \quad (1)$$

where C_0 and C_e (mg/L) are the liquid-phase concentrations of TCP at initial and at equilibrium, respectively. V is the volume of the solution (L) and W is the mass of dry adsorbent used (g).

2.3.1. Effect of TCP initial concentration and agitation time

In order to study the effect of TCP initial concentration and contact time on the adsorption uptake, 100 mL of TCP solutions with initial concentrations of 25–250 mg/L were prepared in a series of 250 mL Erlenmeyer flasks. 0.1 g of the EFB-based activated carbon was added into each flask covered with glass stopper and the flasks were then placed in an isothermal water bath shaker at constant temperature, with rotation speed of 120 rpm, until equilibrium point was reached. In this case, the solution pH was kept original without any pH adjustment.

2.3.2. Effect of solution temperature

The effect of solution temperature on the adsorption process was studied by varying the adsorption temperature at 30, 40 and 50 °C by adjusting the temperature controller of the water bath shaker, while other operating parameters such as activated carbon dosage and rotation speed were remained constant while the solution pH was original without any adjustment.

2.3.3. Effect of solution pH

The effect of solution pH on the TCP removal was examined by varying the initial pH of the solutions from pH 2 to 12. The pH was adjusted using 0.1 M HCl and/or 0.1 M sodium hydroxide (NaOH) and was measured using pH meter (Model Ecoscan, EUTECH Instruments, Singapore). The TCP initial concentration was fixed at 175 mg/L, with activated carbon dosage of 0.1 g/100 mL and solution temperature of 30 °C. The TCP percent removal was calculated using Eq. (2).

$$\text{Romoval}\,(\%) = \frac{C_0 - C_e}{C_0} \times 100 \quad (2)$$

2.4. Batch kinetic studies

The procedure of kinetic adsorption tests was identical to that of batch equilibrium tests, however the aqueous samples were taken at preset time intervals. The concentrations of TCP were similarly measured. The TCP uptake at any time, q_t (mg/g), was calculated by Eq. (3).

$$q_t = \frac{(C_0 - C_t)V}{W} \quad (3)$$

where C_t (mg/L) is the liquid-phase concentration of TCP at any time, t (h).

2.5. Regeneration of activated carbon

The feasibility of regenerating the spent activated carbon saturated with TCP was evaluated using ethanol desorption technique [26]. Initially, batch equilibrium tests were performed on the fresh activated carbons prepared where 100 mL of TCP solution with initial concentration of 200 mg/L were placed in 250 mL Erlenmeyer flasks. 0.1 g of the fresh EFB-based activated carbon was added into the flask and placed in an isothermal water bath shaker at

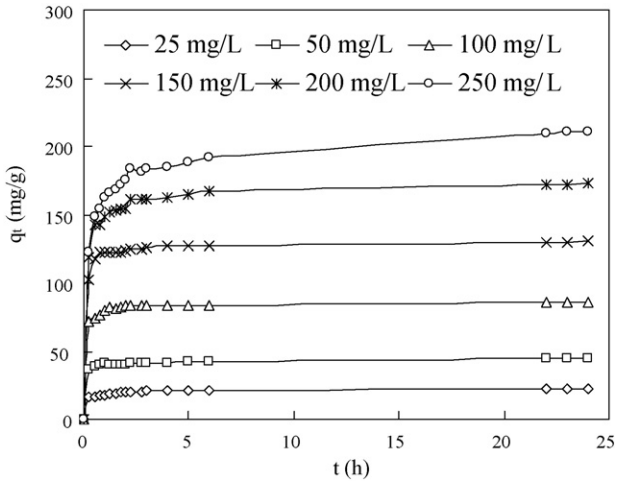

Fig. 1. Effect of agitation time on TCP adsorption on EFB-based activated carbon at various initial concentrations (25–250 mg/L) at 30 °C.

30 °C, with rotation speed of 120 rpm, agitated for 48 h until complete equilibrium was attained. The solution pH was kept original without any pH adjustment. The concentrations were similarly measured using UV–vis spectrophotometer and the concentration of adsorbate adsorbed at equilibrium, C_{ad} (mg/L) was calculated as the difference between the initial and equilibrium concentration ($C_0 - C_e$).

The spent activated carbon was then separated from the solution and washed with deionized water to remove any unsorbed TCP. The sample was then dried at 110 °C in an oven (Model Memmert 600, Germany) and then added into Erlenmeyer flask containing 100 mL of 95 vol.% ethanol for desorption of the TCP. The flask was kept in the isothermal water bath shaker at the same temperature for the same time duration as the adsorption tests. After desorption, the concentrations of TCP desorbed, C_{de} (mg/L) was similarly measured using the UV–vis spectrophotometer. The percent desorption was calculated using Eq. (4).

$$\text{Desorption}\,(\%) = \frac{C_{de}}{C_{ad}} \times 100 \tag{4}$$

3. Results and discussion

3.1. Effect of TCP initial concentration and agitation time on adsorption equilibrium

Fig. 1 shows the effects of agitation time and TCP initial concentration on the TCP uptake on the EFB-based activated carbon at 30 °C. The plots show that the adsorption of TCP increase with time and, at some point in time, it reached a constant value beyond which no more TCP was further removed from the solutions. The adsorption curves are single smooth and continuous leading to saturation. At the equilibrium point, the amount of TCP desorbing from the activated carbon was in a state of dynamic equilibrium with the amount of TCP being adsorbed on the activated carbon. The amount of TCP adsorbed at the equilibrium time reflected the maximum adsorption uptake of the adsorbent under the operating conditions applied. The results revealed that the TCP adsorption was fast at the initial stages of the contact period, and thereafter it became slower near the equilibrium. This phenomenon was due to the fact that a large number of vacant surface sites were available for adsorption during the initial stage, and after a lapse of time, the remaining vacant surface sites were difficult to be occupied due to repulsive forces between the solute molecules on the solid and bulk phases. Similar trend was observed in the adsorption of TCP on activated clay and coconut shell-based activated carbon [2,4]. TCP was adsorbed fast due to high affinity of the interacting groups on the surface of the activated carbon. The high adsorption rate at the beginning of adsorption was due to the adsorption of TCP by the exterior surface of the adsorbent. When saturation was reached at the exterior surface, the TCP molecules entered the pores of adsorbent and were adsorbed by the interior surface of the particles [4,6].

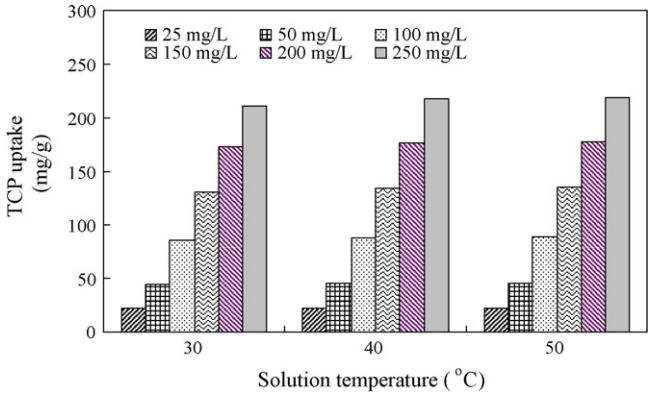

Fig. 2. Effect of solution temperature on TCP uptake at various initial concentrations.

In this study, the adsorption uptake at equilibrium, q_e, increased from 22.49 to 210.79 mg/g with an increase in initial concentration from 25 to 250 mg/L. This was because when the initial concentration increased, the mass transfer driving force would become larger, hence resulting in higher TCP adsorption. At lower initial concentration, the active vacant sites available on the activated carbon were sufficient to adsorb most of the TCP molecules as the ratio of the initial number of the TCP molecules to the vacant sites was low.

It can be seen from Fig. 1 that longer contact times were required by the TCP solutions of higher initial concentrations to reach equilibrium. The contact times needed for TCP solutions with initial concentrations of 25–150 mg/L to reach equilibrium was less than 1 h. However, for TCP solutions of higher initial concentrations (200–250 mg/L), equilibrium times of 5–6 h were required. This observation could be explained by the fact that in the process of adsorption, initially the adsorbate molecules had to first encounter the boundary layer effect and then diffused from the boundary layer film onto adsorbent surface and then finally, they had to diffuse into the porous structure of the adsorbent [27]. This phenomenon took relatively long contact time. Therefore, TCP solutions with higher initial concentrations would take longer contact time to attain equilibrium due to higher amount of TCP molecules to be adsorbed. Radhika and Palanivelu [2] found that the equilibrium time for the adsorption of TCP on coconut shell-based commercial grade activated carbon was 60–210 min for TCP initial concentration of 10–100 mg/L. Denizli et al. [28] reported that for initial concentration of 500 mg/L, amount of TCP adsorbed was very high at the beginning of adsorption, and saturation level was gradually reached within 4 h. Hameed [4] found that the equilibrium time needed for adsorption of TCP on activated clay was almost 30 min for initial concentration below 150 mg/L, and more than 1 h was required for higher concentration. This shows that the adsorption performance of the activated carbon prepared in this study was comparable with the works done by previous researchers.

3.2. Effect of solution temperature on TCP adsorption

Fig. 2 shows the TCP adsorption uptake, q_e (mg/g) on the activated carbon prepared versus the solution temperature at various

initial concentrations (25–250 mg/L). The TCP adsorption uptake was found to increase with increasing solution temperature from 30 to 50 °C for all initial concentrations, indicating the endothermic nature of the adsorption reaction. Increasing the temperature was known to increase the rate of diffusion of the adsorbate molecules across the external boundary layer and in the internal pores of the adsorbent particle, owing to the decrease in the viscosity of the solution [29]. The enhancement in the adsorption capacity might be due to the chemical interaction between adsorbates and adsorbent, creation of some new adsorption sites or the increased rate of intraparticle diffusion of adsorbate molecules into the pores of the activated carbons at higher temperatures [30]. Senthilkumaar et al. [31] also noted similar observations and they suggested that the increase in adsorption capacity with increase in temperature might be due to the possibility of an increase in the porosity and in the total pore volume of the adsorbent, an increase of number of active sites for the adsorption as well as an increase in the mobility of the adsorbate molecules.

3.3. Effect of solution pH on TCP adsorption

Fig. 3 shows the effect of solution pH on the TCP percent removal on the activated carbon prepared. As can be seen from this plot, the TCP removal was found to decrease significantly with increase in initial pH of the solution from pH 2 to 12. In this study, the highest TCP removal was achieved at pH 2, with TCP removal as high as 97.76%, at TCP initial concentration of 175 mg/L. As TCP is a weak acid compound, therefore at acidic pH below the pK_a of TCP, the TCP was undissociated and the dispersion interactions predominated [25]. The unionized species of halogenated organic compounds were high, which did not favour any repulsion between the activated carbon surface and the molecular species of TCP, thereby increased the electrostatic attractions between the TCP molecules and the adsorption sites.

However, at basic pH, the TCP which was a weak acidic electrolyte would be dissociated and therefore the electrostatic repulsions occurred between the negative surface charge and the chlorophenolate anions and between chlorophenolate–chlorophenolate anions in the solutions [25]. Besides, there might be competition between the OH^- ions and the ionic species of TCP, hence reducing the TCP removal. On the whole, the protonated phenolic compounds dominating at low pH were more adsorbable than the ionized forms. Similar trend was reported in the adsorption of TCP on coconut shell-based activated carbon [2] and activated clay [4] as well as adsorption of 4-chlorophenol and 2,4-dichlorophenol on anaerobic granular sludge [1].

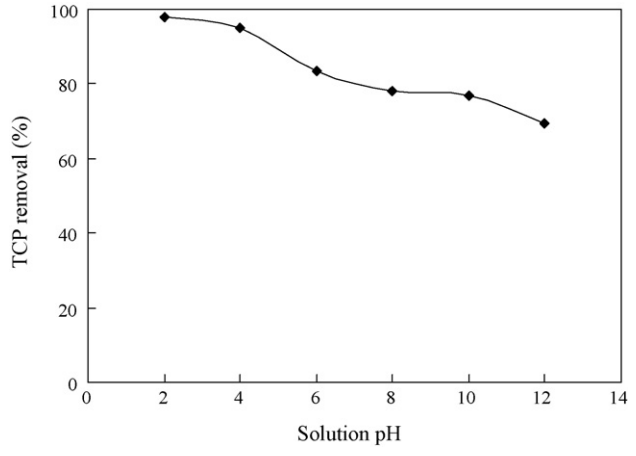

Fig. 3. Effect of solution pH on TCP removal at 30 °C (TCP initial concentration = 175 mg/L).

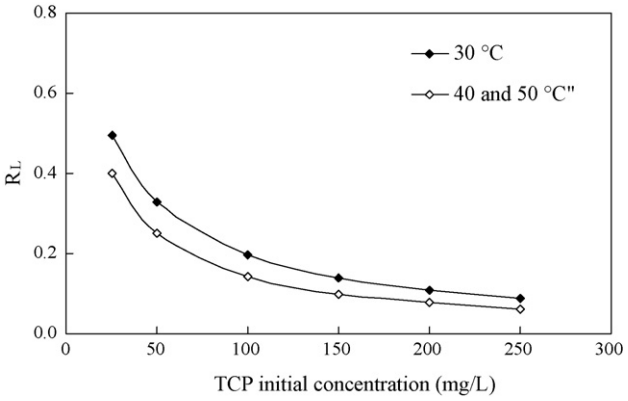

Fig. 4. Effect of TCP initial concentration on separation factor R_L at 30, 40 and 50 °C.

3.4. Adsorption isotherms

In order to optimize the design of an adsorption system, it is important to establish the most appropriate correlation for the equilibrium curves. In this study, five adsorption isotherms: the Langmuir, Freundlich, Temkin, Dubinin–Radushkevich (DR) and Redlich–Peterson (RP) isotherms were applied to fit the equilibrium data of adsorption of TCP on the EFB-based activated carbon. For the Langmuir, Freundlich, Temkin and DR models, the linearized forms of the equations were applied whereas for RP model, the non-linearized equation was applied as this model consisted of three unknown parameters which could only be solved using non-linear regression.

Langmuir isotherm assumes monolayer adsorption onto a surface containing a finite number of adsorption sites of uniform strategies of adsorption with no transmigration of adsorbate in the plane of surface [32]. The linear form of Langmuir isotherm equation is given as:

$$\frac{C_e}{q_e} = \frac{1}{Q_o K_L} + \frac{1}{Q_o} C_e \quad (5)$$

where C_e (mg/L) is the equilibrium concentration of the TCP, q_e (mg/g) is the amount of TCP adsorbed per unit mass of adsorbent, Q_o and K_L are Langmuir constants related to adsorption capacity and rate of adsorption, respectively. When C_e/q_e is plotted against C_e, a straight line with slope of $1/Q_o$ and intercept of $1/Q_o K_L$ is obtained.

The essential characteristics of Langmuir isotherm can be expressed by a dimensionless constant called separation factor or equilibrium parameter, R_L, defined by Weber and Chakkravorti [32] as:

$$R_L = \frac{1}{1 + K_L C_o} \quad (6)$$

The parameter R_L indicates the shape of isotherm as follows:

Value of R_L	Type of isotherm
$R_L > 1$	Unfavourable
$R_L = 1$	Linear
$0 < R_L < 1$	Favourable
$R_L = 0$	Irreversible

Fig. 4 represents the calculated R_L values versus the initial concentration of TCP at 30, 40 and 50 °C. All the R_L values were between 0 and 1, indicating that the adsorption of TCP on the activated carbon was favourable at the conditions being studied. However, the R_L

values decreased as the initial concentration increased from 25 to 250 mg/L. This indicated that the adsorption was more favourable at higher initial concentration.

Freundlich model is an empirical equation based on sorption on a heterogeneous surfaces or surfaces supporting sites of varied affinities. It is assumed that the stronger binding sites are occupied first and that the binding strength decreases with the increasing degree of site occupation [33]. The well-known logarithmic form of Freundlich isotherm is given by the following equation:

$$\log q_e = \log K_F + \left(\frac{1}{n}\right) \log C_e \quad (7)$$

where K_F and n are Freundlich constants with n giving an indication of how favourable the adsorption process and K_F (mg/g (L/mg)$^{1/n}$) is the adsorption capacity of the adsorbent. K_F can be defined as the adsorption or distribution coefficient and represents the quantity of dye adsorbed onto activated carbon for a unit equilibrium concentration. The slope of $1/n$ ranging between 0 and 1 is a measure of adsorption intensity or surface heterogeneity, becoming more heterogeneous as its value gets closer to zero [34]. The value of $1/n$ below one indicates a normal Langmuir isotherm while $1/n$ above one is indicative of cooperative adsorption. The plot of $\log q_e$ versus $\log C_e$ gave a straight line with slope of $1/n$ and intercept of $\log K_F$.

Temkin isotherm [35] contains a factor that explicitly takes into account the adsorbent–adsorbate interactions. The heat of adsorption of all the molecules in the layer would decrease linearly with coverage due to adsorbent–adsorbate interactions. The adsorption is characterized by a uniform distribution of binding energies, up to some maximum binding energy. The Temkin isotherm is expressed as:

$$q_e = \left(\frac{RT}{b_T}\right) \ln(AC_e) \quad (8)$$

where $RT/b_T = B$ (J/mol), which is the Temkin constant related to heat of sorption whereas A (L/g) is the equilibrium binding constant corresponding to the maximum binding energy. R (8.314 J/mol K) is the universal gas constant and T (K) is the absolute solution temperature.

Dubinin–Radushkevich isotherm is defined as [36]:

$$q_e = q_s \exp(-B_{DR}\varepsilon^2) \quad (9)$$

where ε can be correlated as:

$$\varepsilon = RT \ln\left[1 + \frac{1}{C_e}\right] \quad (10)$$

The constant B_{DR} gives the mean free energy E of sorption per molecule of the sorbate when it is transferred to the surface of the solid from infinity in the solution and can be computed by using the following relationship:

$$E = \left[\frac{1}{\sqrt{2B_{DR}}}\right] \quad (11)$$

where R is the gas constant (8.314 J/mol K) and T is the absolute temperature (K). A plot of $\ln q_e$ versus ε^2 enables the constants E and q_s to be determined from the slope and intercept, respectively.

The Redlich–Peterson equation [37] is widely used as a compromise between Langmuir and Freundlich systems. This model has three parameters and incorporates the advantageous significance of both models. RP model can be represented as follows:

$$q_e = \frac{K_{RP}C_e}{1 + (\alpha C_e)^{\beta}} \quad (12)$$

where K_{RP} (L/g) and α (L/mg)$^{\beta}$ are RP isotherm constants whereas β is the exponent which lies between 0 and 1. RP model has two limiting cases, when $\beta = 1$, the Langmuir equation results whereas when $\beta = 0$, R–P equation transforms to Henry's law equation.

All the correlation coefficient, R^2 values and the constants obtained from the five isotherm models applied for adsorption of TCP at 30, 40 and 50 °C on the activated carbon derived from EFB are summarized in Table 1. The Freundlich and RP models gave the highest R^2 values which were greater than 0.96 at all the three temperatures studied, showing that the adsorption of TCP on the activated carbon was best described by these two models. The β constant obtained for the adsorption process at 30, 40 and 50 °C were 0.20, 0.21 and 0.37, respectively. All the $1/n$ values obtained from the Freundlich model were below one at all solution temperatures, representing that adsorption of TCP on the activated carbon was favourable. The results agreed with the works carried out by previous researchers which reported that the Freundlich model gave a better fit than the Langmuir model on the adsorption of chlorophenols using different adsorbents, such as activated clay [4], fungal mycelia [38] and surfactant-modified natural zeolite [39]. This suggested that some heterogeneity on the surfaces or pores of the activated carbon played the role in TCP adsorption. However, some researchers revealed that the adsorption of chlorophenols on adsorbents such as rice straw-based activated carbon [10], anaerobic granular sludge [1] and corncob-based activated carbon [40] were better represented by the Langmuir isotherm whereas the best fit was achieved for adsorption of *p*-chlorophenol on cork-based activated carbon with the RP model [41]. Table 2 lists the comparison of the maximum monolayer adsorption capacity of various types of chlorophenols on various adsorbents. The activated carbon prepared in this work showed relatively large TCP adsorption capacity of 500 mg/g, as compared to some previous works reported in the literature.

3.5. Adsorption kinetic studies

The kinetics of adsorption describes the rate of adsorbate uptake on activated carbon and it controls the equilibrium time. The pseudo-first-order, pseudo-second-order kinetic models and Elovich equation were applied to study the kinetics of the adsorption process whereas the intraparticle diffusion model was further tested to determine the diffusion mechanism of the adsorption system.

3.5.1. Pseudo-first-order kinetic model

The pseudo-first-order kinetic model has been widely used to predict sorption kinetics. The model given by Langergren and Svenska [42] is defined as:

$$\ln(q_e - q_t) = \ln q_e - k_1 t \quad (13)$$

where q_e and q_t (mg/g) are the amounts of adsorbate adsorbed at equilibrium and at any time, t (h), respectively and k_1 (1/h) is the adsorption rate constant. The plot of $\ln(q_e - q_t)$ versus t as shown in Fig. 5 gave the slope of k_1 and intercept of $\ln q_e$. The values of k_1 and correlation coefficient, R^2 obtained from the plots for adsorption of TCP on the activated carbon at 30 °C are given in Table 3. The R^2 values were relatively small, which varied from 0.479 to 0.801 for TCP initial concentration of 25–250 mg/L. Besides, the experimental q_e values did not agree with the calculated values obtained from the linear plots. This shows that the adsorption of TCP on the activated carbon is not a first-order reaction.

Table 1
Langmuir, Freundlich, Temkin, Dubinin–Radushkevich and Redlich–Peterson isotherm model constants and correlation coefficients

Isotherms	Solution temperature (K)	Constants		R^2
		Q_o (mg/g)	K_L (L/mg)	
Langmuir, $\frac{C_e}{q_e} = \frac{1}{Q_o K_L} + \frac{1}{Q_o} C_e$	303	500.00	0.04	0.839
	313	555.56	0.06	0.618
	323	588.24	0.06	0.695
Isotherms	Solution temperature (K)	Constants		R^2
		K_F (mg/g (L/mg)$^{1/n}$)	$1/n$	
Freundlich, $\log q_e = \log K_F + \left(\frac{1}{n}\right) \log C_e$	303	22.04	0.80	0.998
	313	31.48	0.82	0.969
	323	35.52	0.84	0.977
Isotherms	Solution temperature (K)	Constants		R^2
		A (L/g)	B	
Temkin, $q_e = \left(\frac{RT}{b}\right) \ln(AC_e)$	303	1.00	64.97	0.907
	313	1.46	69.56	0.917
	323	1.65	72.36	0.934
Isotherms	Solution temperature (K)	Constants		R^2
		q_s (mg/g)	E (J/mol)	
Dubinin–Radushkevich, $q_e = q_s \exp(-B\varepsilon^2)$	303	135.73	845.15	0.806
	313	158.86	1000.00	0.912
	323	163.02	1118.03	0.923
Isotherms	Solution temperature (K)	Constants		R^2
		K_{RP} (L/g)	α (L/mg)$^{\beta}$	
Redlich–Peterson, $q_e = \frac{K_{RP} C_e}{1+(\alpha C_e)^{\beta}}$	303	85.75	380.80	0.998
	313	150.40	584.40	0.983
	323	66.74	0.51	0.979

Table 2
Comparison of maximum monolayer adsorption capacity of various chlorophenols on various adsorbents

Adsorbent	Adsorbate	Maximum monolayer adsorption capacity (mg/g)	References
EFB-based activated carbon	2,4,6-Trichlorophenol	500.00	This work
Commercial grade coconut shell-based activated carbon	2,4,6-Trichlorophenol	112.35	[2]
Coconut husk-based activated carbon	2,4,6-Trichlorophenol	716.10	[58]
Activated clay	2,4,6-Trichlorophenol	123.46	[4]
Coir pith carbon	2,4-Dichlorophenol	19.12	[11]
Palm pith carbon	2,4-Dichlorophenol	19.16	[57]
Anaerobic granular sludge	4-Chlorophenol	6.32	[1]
Rice straw-based carbon	3-Chlorophenol	14.20	[10]

3.5.2. Pseudo-second-order kinetic model

The pseudo-second-order equation [43] based on equilibrium adsorption is expressed as:

$$\frac{t}{q} = \frac{1}{k_2 q_e^2} + \frac{1}{q_e} t \quad (14)$$

where k_2 (g/mg h) is the rate constant of second-order adsorption. The linear plot of t/q_t versus t gave $1/q_e$ as the slope and $1/k_2 q_e^2$ as the intercept. This procedure is more likely to predict the behavior over the whole range of adsorption. The linear plot of t/q_t versus t, as shown in Fig. 6, shows a good agreement between the experimental and the calculated q_e values (Table 3). Besides, the correlation coefficient values for the second-order kinetic model were almost equal to unity for all TCP concentrations, indicating the applicability of the second-order kinetic model to describe the adsorption process of TCP on the prepared activated carbon.

Table 3
Pseudo-first-order model, pseudo-second-order model and Elovich equation constants and correlation coefficients for adsorption of TCP on EFB-based activated carbon at 30 °C

Initial TCP concentration (mg/L)	$q_{e,exp}$ (mg/g)	Pseudo-first-order kinetic model			Pseudo-second-order kinetic model			Elovich equation			
		$q_{e,cal}$ (mg/g)	k_1 (1/h)	R^2	$q_{e,cal}$ (mg/g)	k_2 (g/mg h)	R^2	$q_{e,cal}$ (mg/g)	$(1/b)\ln(ab)$ (mg/g)	$1/b$ (mg/g)	R^2
25	22.49	11.33	0.82	0.768	20.75	0.40	0.997	19.61	18.29	1.90	0.953
50	44.66	13.77	0.77	0.479	40.65	1.51	0.999	40.81	39.63	1.70	0.762
100	86.32	32.79	1.32	0.801	85.47	0.17	0.999	83.27	79.11	6.00	0.950
150	130.04	38.90	1.15	0.626	126.58	0.21	0.999	126.36	120.12	9.00	0.771
200	172.48	76.45	0.89	0.711	161.29	0.08	0.999	157.54	146.45	16.00	0.898
250	210.79	118.99	0.70	0.764	185.19	0.04	0.999	176.55	160.03	23.83	0.974

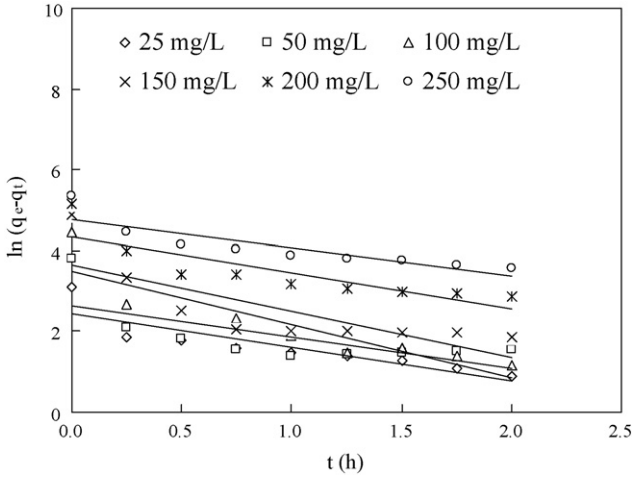

Fig. 5. Pseudo-first-order kinetics for adsorption of TCP on EFB-based activated carbon at 30 °C.

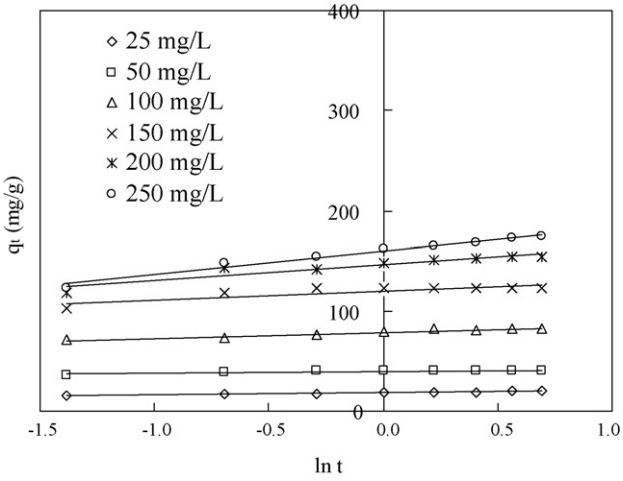

Fig. 7. Plot of Elovich equation for adsorption of TCP on EFB-based activated carbon at 30 °C.

3.5.3. Elovich equation

Elovich equation is one of the most useful models for describing chemisorption, which is given as [44]:

$$q_t = \left(\frac{1}{b}\right) \ln(ab) + \frac{1}{b} \ln t \tag{15}$$

where a (mg/g h) is the initial sorption rate and b (g/mg) is related to the extent of surface coverage and activation energy for chemisorption. The parameters $(1/b)$ and $(1/b)\ln(ab)$ can be obtained from the slope and intercept of the linear plot of q_t versus $\ln t$, as shown in Fig. 7. The value of $(1/b)$ is indicative of the number of sites available for adsorption while the $(1/b)\ln(ab)$ is the adsorption quantity when $\ln t$ is equal to zero; i.e., the adsorption quantity when t is 1 h. This value is helpful in understanding the adsorption behavior of the first step [45]. The R^2 values obtained from Elovich equation was in the range of 0.762–0.974 for TCP initial concentration of 25–250 mg/L (Table 3). The q_e values calculated from Elovich equation agreed quite well with the experimental values.

3.5.4. Validity of kinetic model

The applicability of the three kinetic models above to describe the adsorption process was further validated by the normalized standard deviation, Δq_e (%), which is defined as:

$$\Delta q_t\,(\%) = 100\sqrt{\frac{\sum[(q_{t,\mathrm{exp.}} - q_{t,\mathrm{cal.}})/q_{t,\mathrm{exp}}]^2}{N-1}} \tag{16}$$

where N is the number of data points, $q_{t,\mathrm{exp}}$ and $q_{t,\mathrm{cal}}$ (mg/g) are the experimental and calculated adsorption uptake, respectively.

The Δq_t obtained for the pseudo-first-order kinetic model was ranged from 10.62% to 17.12% for TCP initial concentration ranging from 25 to 250 mg/L, which was relatively high as compared to the Δq_t values of 0.05–0.72% and 0.11–0.79% obtained for the pseudo-second-order kinetic model and Elovich equation, respectively. Based on the highest R^2 values which approached unity and the lowest Δq_t values, the pseudo-second-order model was therefore the most suitable equation to describe the adsorption kinetics of TCP on the activated carbon prepared. This suggested that the overall rate of the adsorption process was controlled by chemisorption which involved valency forces through sharing or exchange of electrons between the sorbent and sorbate [46]. From the literature, the adsorption of TCP on activated clay [4] and coconut shell-based activated carbon [2] as well as adsorption of 2-chlorophenol on coir pith carbon [47] were as well found to be best represented by the pseudo-second-order model.

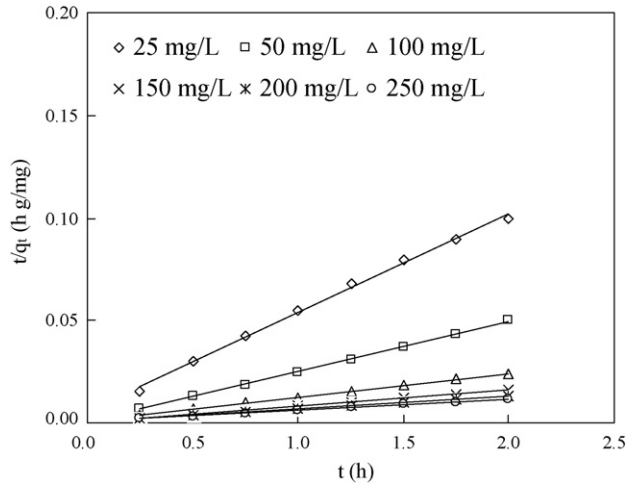

Fig. 6. Pseudo-second-order kinetics for adsorption of TCP on EFB-based activated carbon at 30 °C.

3.6. Adsorption mechanism

As the above kinetic models were not able to identify the diffusion mechanism, thus intraparticle diffusion model based on the theory proposed by Weber and Morris [48] was tested. It is an empirically found functional relationship, common to the most adsorption processes, where uptake varies almost proportionally with $t^{1/2}$ rather than with the contact time t. According to this theory:

$$q_t = k_{\mathrm{pi}} t^{1/2} + C_i \tag{17}$$

where k_{pi} (mg/g h$^{1/2}$), the rate parameter of stage i, is obtained from the slope of the straight line of q_t versus $t^{1/2}$ (Fig. 8). C_i, the intercept of stage i, gives an idea about the thickness of boundary layer, i.e., the larger the intercept, the greater the boundary layer effect. If intraparticle diffusion occurs, then q_t versus $t^{1/2}$ will be linear and if the plot passes through the origin, then the rate limiting process is only due to the intraparticle diffusion. Otherwise, some other mechanism along with intraparticle diffusion is also involved.

Table 4
Intraparticle diffusion model constants and correlation coefficients for adsorption of TCP on EFB-based activated carbon at 30 °C

Initial TCP concentration (mg/L)	Intraparticle diffusion model								
	k_{p1} (mg/g h$^{1/2}$)	k_{p2} (mg/g h$^{1/2}$)	k_{p3} (mg/g h$^{1/2}$)	C_1	C_2	C_3	$(R_1)^2$	$(R_2)^2$	$(R_3)^2$
25	32.14	4.33	–	0	13.76	–	1.00	0.987	–
50	73.15	3.46	–	0	36.00	–	1.00	0.630	–
100	143.54	16.71	4.57	0	62.60	76.40	1.00	0.962	0.659
150	204.69	55.54	2.14	0	75.70	120.31	1.00	0.954	0.776
200	237.10	115.55	19.55	0	60.77	127.95	1.00	1.00	0.925
250	245.72	123.53	37.94	0	61.10	122.21	1.00	1.00	0.983

For intraparticle diffusion plots, the first, sharper region is the instantaneous adsorption or external surface adsorption. The second region is the gradual adsorption stage where intraparticle diffusion is the rate limiting. In some cases, the third region exists, which is the final equilibrium stage where intraparticle diffusion starts to slow down due to the extremely low adsorbate concentrations left in the solutions [49]. Referring to Fig. 8, for all initial concentrations, the first stage was completed within the first 15 min and the second stage of intraparticle diffusion control was then attained. The third stage only occurred for higher TCP initial concentration of 100–250 mg/L. The different stages of rates of adsorption observed indicated that the adsorption rate was initially faster and then slowed down when the time increased.

As can be seen from Fig. 8, the linear lines of the second and third stages did not pass through the origin and this deviation from the origin or near saturation might be due to the difference in the mass transfer rate in the initial and final stages of adsorption [50]. It shows that intraparticle diffusion was not the only rate limiting mechanism in the adsorption process. The values of k_{pi}, C_i and correlation coefficient, R^2 obtained for the plots are given in Table 4. The k_{pi} values were found to be generally increased with the increasing TCP initial concentration which was due to the greater driving force [51].

Kinetic data as obtained by the batch method has been treated by the expressions given by Boyd et al. [52], which is in accordance with the observations of Reichenberg [53]. The three sequential steps in the adsorption are:

i. Film diffusion, where adsorbate ions travel towards the external surface of the adsorbent.
ii. Particle diffusion, where adsorbate ions travel within the pores of the adsorbent excluding a small amount of adsorption that occurs on the exterior surface of the adsorbent.
iii. Adsorption of the adsorbate ions on the interior surface of the adsorbent.

The third step is considered to be very fast thus it cannot be treated as rate limiting step. If external transport > internal transport, rate is governed by particle diffusion. If external transport < internal transport, rate is governed by film diffusion and if external transport ≈ internal transport, the transport of adsorbate ions to the boundary may not be possible at a significant rate thus, formation of a liquid film surrounding the adsorbent particles takes place through the proper concentration gradient [54].

In order to predict the actual slow step involved in the adsorption process, the kinetic data were further analyzed using the Boyd model given by Eq. (18).

$$B_t = -0.4977 - \ln(1 - F) \tag{18}$$

F represents the fraction of solute adsorbed at any time, t (h), as calculated using Eq. (19).

$$F = \frac{q_t}{q_0} \tag{19}$$

The calculated B_t values were plotted against time t (h), as shown in Fig. 9. The linear lines for all TCP initial concentrations did no pass through the origin and the points were scattered. This indicated that the adsorption of TCP on the prepared activated carbon was mainly governed by external mass transport where particle diffusion was the rate limiting step [55].

3.7. Adsorption thermodynamics

The concept of thermodynamic assumes that in an isolated system where energy cannot be gained or lost, the entropy change is the driving force [56]. The thermodynamic parameters that must

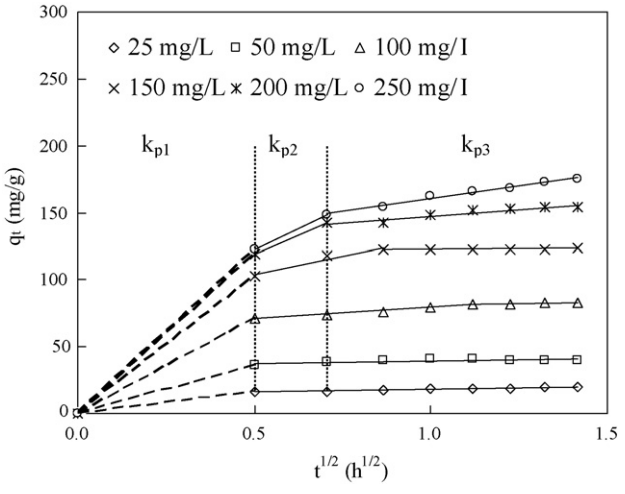

Fig. 8. Plot of intraparticle diffusion model for adsorption of TCP on EFB-based activated carbon at 30 °C.

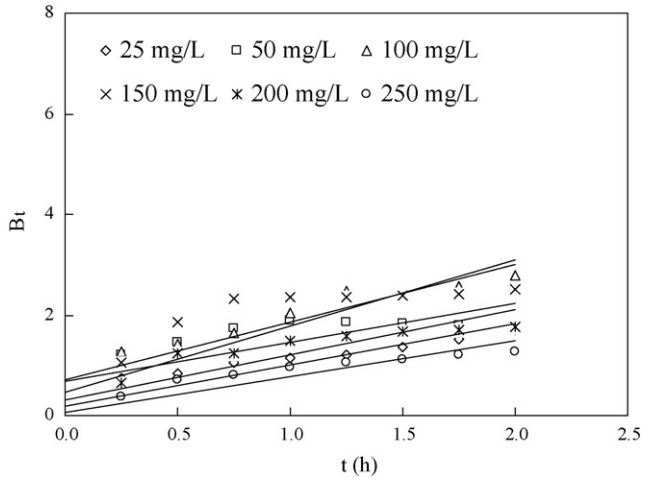

Fig. 9. Boyd plot for adsorption of TCP on EFB-based activated carbon at 30 °C.

Table 5
Thermodynamic parameters for adsorption of TCP on EFB-based activated carbon

ΔH° (kJ/mol)	ΔS° (J/mol K)	E_a (kJ/mol)	ΔG° (kJ/mol)		
			303 K	313 K	323 K
15.65	25.59	1.52	8.05	7.32	7.56

be considered to determine the adsorption processes were changes in standard enthalpy (ΔH°), standard entropy (ΔS°), standard free energy (ΔG°) due to transfer of unit mole of solute from solution onto the solid–liquid interface, as well activation energy of adsorption (E_a). The value of ΔH° and ΔS° can be computed using the following equation:

$$\ln K_L = \frac{\Delta S^\circ}{R} - \frac{\Delta H^\circ}{RT} \quad (20)$$

where R (8.314 J/mol K) is the universal gas constant, T (K) is the absolute solution temperature and K_L (L/mg) is the Langmuir isotherm constant.

The values of ΔH° and ΔS° can be calculated, respectively from the slope and intercept of the van't Hoff plot of $\ln K_L$ versus $1/T$ (figure not shown). ΔG° can then be calculated using the relation below:

$$\Delta G^\circ = -RT \ln K_L \quad (21)$$

Arrhenius equation has been applied to evaluate the activation energy of adsorption representing the minimum energy that reactants must have for the reaction to proceed, as shown by the following relationship:

$$\ln k_2 = \ln A - \frac{E_a}{RT} \quad (22)$$

where k_2 (g/mg h) is the rate constant obtained from the pseudo-second-order kinetic model, E_a (kJ/mol) is the Arrhenius activation energy of adsorption and A is the Arrhenius factor. When $\ln k_2$ is plotted against $1/T$, a straight line with slope of $-E_a/R$ is obtained (figure not shown).

The calculated values of ΔH°, ΔS°, ΔG° and E_a for adsorption of TCP on the activated carbon prepared are listed in Table 5. The positive ΔH° value obtained indicated that the adsorption process was endothermic in nature. This finding was consistent with the results obtained earlier where the TCP uptake increased with increasing solution temperature. The adsorption reaction for the endothermic processes could be due to the increase in temperature increased the rate of diffusion of the adsorbate molecules across the external boundary layer and in the internal pores of the adsorbent particle, owing to the decrease in the viscosity of the solution [29]. Senthilkumaar et al. [31] in the other hand suggested that the increase in adsorption uptake with increase in temperature was due to the possibility of an increase in the mobility of the adsorbate molecules.

The positive values of ΔS° obtained showed the affinity of the activated carbon for TCP and the increasing randomness at the solid–solution interface with some structural changes in the adsorbates and adsorbents during the adsorption process whereas the positive values of ΔG° obtained indicated the non-spontaneous nature of the adsorption process at the range of temperatures being studied. This phenomenon had also been observed in the adsorption of 2,4-dichlorophenol on palm pith carbon [57].

3.8. Regeneration of spent activated carbon

The feasibility of regenerating the spent activated carbon saturated with TCP was evaluated using ethanol desorption technique. It was found that the TCP percent desorption was as high as 99.6%. It was reported in the literature that by using ethanol desorption, the regeneration efficiency of waste tires-based activated carbons for phenol was 35–45% [26] whereas NaOH desorption method was reported to give 78% and 85.4% of parachlorophenol and TCP desorption, respectively from spent commercial activated carbons from Anand Carbons, India [2]. Thus, ethanol desorption technique was shown to be a promising way to regenerate the spent activated carbon prepared in this study as nearly all the adsorption sites could be recovered from the regenerated activated carbon.

4. Conclusions

The present investigation showed that EFB-based activated carbon was a promising low cost adsorbent to be used in the removal of TCP from aqueous solutions over a wide range of concentrations. Adsorption of TCP was found to increase with increase in agitation time, TCP initial concentration and solution temperature. Acidic solution pH was proved to be more favourable for adsorption of TCP on the activated carbon. The equilibrium data were best described by the Freundlich and Redlich–Peterson isotherm models. The kinetics of the adsorption process was found to follow the pseudo-second-order kinetic model. From Boyd plot, the adsorption of TCP on the prepared activated carbon was shown to be mainly governed by particle diffusion. The positive ΔH° value indicated that the adsorption process was endothermic in nature. Ethanol desorption technique was shown to be a promising way to regenerate the spent activated carbon prepared in this study by giving relatively high TCP desorption of 99.6%.

Acknowledgments

The authors acknowledge the research grant provided by Universiti Sains Malaysia under The Fundamental Research Grant Scheme (FRGC) (grant no. 203/PJKIMIA/6070015) that resulted in this article.

Appendix A

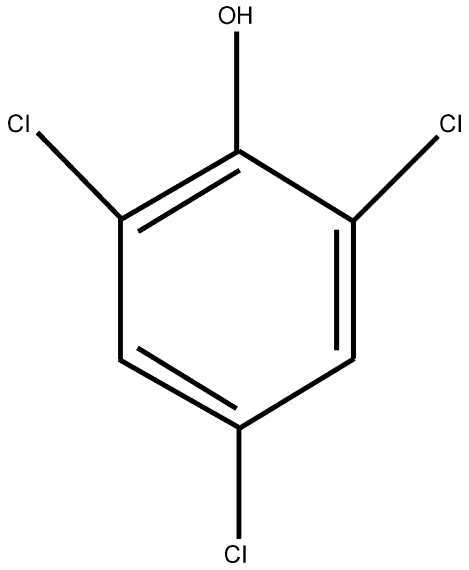

References

[1] R. Gao, J. Wang, Effects of pH and temperature on isotherm parameters of chlorophenols biosorption to anaerobic granular sludge, J. Hazard. Mater. 145 (2007) 398–403.

[2] M. Radhika, K. Palanivelu, Adsorptive removal of chlorophenols from aqueous solution by low cost adsorbent-Kinetics and isotherm analysis, J. Hazard. Mater. B138 (2006) 116–124.
[3] S. Chaliha, K.G. Bhattacharyya, Catalytic wet oxidation of 2-chlorophenol, 2,4-dichlorophenol and 2,4,6-trichlorophenol in water with Mn(II)-MCM41, Chem. Eng. J. 139 (2008) 575–588.
[4] B.H. Hameed, Equilibrium and kinetics studies of 2,4,6-trichlorophenol adsorption onto activated clay, Colloids Surf. A: Physicochem. Eng. Aspects 307 (2007) 45–52.
[5] Y.M. Tzou, S.L. Wang, J.C. Liu, Y.Y. Huang, J.H. Chen, Removal of 2,4,6-trichlorophenol from a solution by humic acids repeatedly extracted from a peat soil, J. Hazard. Mater. 152 (2008) 812–819.
[6] S.G. Poulopoulos, M. Nikolaki, D. Karampetsos, C.J. Philippopoulos, Photochemical treatment of 2-chlorophenol aqueous solutions using ultraviolet radiation, hydrogen peroxide and photo-Fenton reaction, J. Hazard. Mater. 153 (2008) 582–587.
[7] S. Andini, R. Cioffi, F. Colangelo, F. Montagnaro, L. Santoro, Adsorption of chlorophenol, chloroaniline and methylene blue on fuel oil fly ash, J. Hazard. Mater. 157 (2008) 599–604.
[8] B.H. Hameed, A.A. Rahman, Removal of phenol from aqueous solutions by adsorption onto activated carbon prepared from biomass material, J. Hazard. Mater. 160 (2008) 576–581.
[9] K.P. Singh, A. Malik, S. Sinha, P. Ojha, Liquid-phase adsorption of phenols using activated carbons derived from agricultural waste material, J. Hazard. Mater. 150 (2008) 626–641.
[10] S.L. Wang, Y.M. Tzou, Y.H. Lu, G. Sheng, Removal of 3-chlorophenol from water using rice-straw-based carbon, J. Hazard. Mater. 147 (2007) 313–318.
[11] C. Namasivayam, D. Kavitha, Adsorptive removal of 2,4-dichlorophenol from wastewater by low-cost carbon from agricultural solid waste: coconut coir pith, Sep. Sci. Technol. 39 (2004) 1407–1425.
[12] F.J. Guymont, in: I.H. Suffet, M.J. McGuire (Eds.), Activated Carbon Adsorption of Organics from Aqueous Phase, vol. 2, Ann Arbor Science, Ann Arbor, MI, 1984 (Chapter 23).
[13] E. Demirbas, M. Kobya, A.E.S. Konukman, Error analysis of equilibrium studies for the almond shell activated carbon adsorption of Cr(VI) from aqueous solutions, J. Hazard. Mater. 154 (2008) 787–794.
[14] B. Cabal, T. Budinova, C.O. Ania, B. Tsyntsarski, J.B. Parra, B. Petrova, Adsorption of naphthalene from aqueous solution on activated carbons obtained from bean pods, J. Hazard. Mater. 161 (2009) 1150–1156.
[15] D. Mohan, K.P. Singh, V.K. Singh, Wastewater treatment using low cost activated carbons derived from agricultural byproducts—a case study, J. Hazard. Mater. 152 (2008) 1045–1053.
[16] J. Jaramillo, V. Gómez-Serrano, P.M. Álvarez, Enhanced adsorption of metal ions onto functionalized granular activated carbons prepared from cherry stones, J. Hazard. Mater. 161 (2009) 670–676.
[17] A. El Nemr, A. Khaled, O. Abdelwahab, A. El-Sikaily, Treatment of wastewater containing toxic chromium using new activated carbon developed from date palm seed, J. Hazard. Mater. 152 (2008) 263–275.
[18] N. Thinakaran, P. Baskaralingam, M. Pulikesi, P. Panneerselvam, S. Sivanesan, Removal of Acid Violet 17 from aqueous solutions by adsorption onto activated carbon prepared from sunflower seed hull, J. Hazard. Mater. 151 (2008) 316–322.
[19] Y. Önal, C. Akmil-Başar, Ç. Sarıcı-Özdemir, Elucidation of the naproxen sodium adsorption onto activated carbon prepared from waste apricot: kinetic, equilibrium and thermodynamic characterization, J. Hazard. Mater. 148 (2007) 727–734.
[20] I.A.W. Tan, B.H. Hameed, A.L. Ahmad, Equilibrium and kinetic studies on basic dye adsorption by oil palm fibre activated carbon, Chem. Eng. J. 127 (2007) 111–119.
[21] B.H. Hameed, A.T.M. Din, A.L. Ahmad, Adsorption of methylene blue onto bamboo-based activated carbon: kinetics and equilibrium studies, J. Hazard. Mater. 141 (2007) 819–825.
[22] R.L. Tseng, Physical and chemical properties and adsorption type of activated carbon prepared from plum kernels by NaOH activation, J. Hazard. Mater. 147 (2007) 1020–1027.
[23] I.A.W. Tan, B.H. Hameed, A.L. Ahmad, Optimization of preparation conditions for activated carbons from coconut husk using response surface methodology, Chem. Eng. J. 137 (2008) 462–470.
[24] I.A.W. Tan, A.L. Ahmad, B.H. Hameed, Preparation of activated carbon from coconut husk: optimization study on removal of 2,4,6-trichlorophenol using response surface methodology, J. Hazard. Mater. 153 (2008) 709–717.
[25] O. Hamdaoui, E. Naffrechoux, Modeling of adsorption isotherms of phenol and chlorophenols onto granular activated carbon: part I. Two-parameter models and equations allowing determination of thermodynamic parameters, J. Hazard. Mater. 147 (2007) 381–394.
[26] W. Tanthapanichakoon, P. Ariyadejwanich, P. Japthong, K. Nakagawa, S.R. Mukai, H. Tamon, Adsorption-desorption characteristics of phenol and reactive dyes from aqueous solution on mesoporous activated carbon prepared from waste tires, Water Res. 39 (2005) 1347–1353.
[27] D.S. Faust, M.O. Aly, Chemistry of Wastewater Treatment, Butterworths, Boston, 1983.
[28] A. Denizli, N. Cihangir, N. Tüzmen, G. Alsancak, Removal of chlorophenols from aquatic systems using the dried and dead fungus *Pleurotus sajor caju*, Bioresour. Technol. 96 (2005) 59–62.
[29] S. Wang, Z.H. Zhu, Effects of acidic treatment of activated carbons on dye adsorption, Dyes Pigments 75 (2007) 306–314.
[30] T. Karthikeyan, S. Rajgopal, L.R. Miranda, Chromium(VI) adsorption from aqueous solution by *Hevea Brasilinesis* sawdust activated carbon, J. Hazard. Mater. 124 (2005) 192–199.
[31] S. Senthilkumaar, P. Kalaamani, K. Porkodi, P.R. Varadarajan, C.V. Subburaam, Adsorption of dissolved reactive red dye from aqueous phase onto activated carbon prepared from agricultural waste, Bioresour. Technol. 97 (2006) 1618–1625.
[32] T.W. Weber, R.K. Chakkravorti, Pore and solid diffusion models for fixed-bed adsorbers, AlChE J. 20 (1974) 228–238.
[33] H.M.F. Freundlich, Over the adsorption in solution, J. Phys. Chem. 57 (1906) 385–470.
[34] F. Haghseresht, G. Lu, Adsorption characteristics of phenolic compounds onto coal-reject-derived adsorbents, Energy Fuels 12 (1998) 1100–1107.
[35] M.I. Temkin, V. Pyzhev, Kinetics of ammonia synthesis on promoted iron catalyst, Acta Physiochim. URSS 12 (1940) 327–356.
[36] S. Rengaraj, Y. Kim, C.K. Joo, K. Choi, J. Yi, Batch adsorptive removal of copper ions in aqueous solutions by ion exchange resins: 1200H and IRN97H, Korean J. Chem. Eng. 21 (2004) 187–194.
[37] O. Redlich, D.L. Peterson, A useful adsorption isotherm, J. Phys. Chem. 63 (1959) 1024–1029.
[38] J. Wu, H.Q. Yu, Biosorption of phenol and chlorophenols from aqueous solutions by fungal mycelia, Process Biochem. 41 (2006) 44–49.
[39] A. Kuleyin, Removal of phenol and 4-chlorophenol by surfactant-modified natural zeolite, J. Hazard. Mater. 144 (2007) 307–315.
[40] R.L. Tseng, S.K. Tseng, F.C. Wu, Preparation of high surface area carbons from Corncob with KOH etching plus CO_2 gasification for the adsorption of dyes and phenols from water, Colloids Surf. A: Physicochem. Eng. Aspects 279 (2006) 69–78.
[41] P.A.M. Mourão, P.J.M. Carrott, M.M.L. Ribeiro Carrott, Application of different equations to adsorption isotherms of phenolic compounds on activated carbons prepared from cork, Carbon 44 (2006) 2422–2429.
[42] S. Langergren, B.K. Svenska, Zur theorie der sogenannten adsorption geloester stoffe, Veternskapsakad Handlingar 24 (4) (1898) 1–39.
[43] Y.S. Ho, G. McKay, The kinetics of sorption of basic dyes from aqueous solutions by sphagnum moss peat, Can. J. Chem. Eng. 76 (1998) 822–826.
[44] M. Ozacar, I.A. Sengil, A kinetic study of metal complex dye sorption onto pine sawdust, Process Biochem. 40 (2005) 565–572.
[45] R.L. Tseng, Mesopore control of high surface area NaOH-activated carbon, J. Colloid Interface Sci. 303 (2006) 494–502.
[46] Y.S. Ho, G. McKay, Pseudo-second order model for sorption processes, Process Biochem. 34 (1999) 451–465.
[47] C. Namasivayam, D. Kavitha, Adsorptive removal of 2-chlorophenol by low-cost coir pith carbon, J. Hazard. Mater. 98 (2003) 257–274.
[48] W.J. Weber, J.C. Morris, In: Proc. Int. Conf. Water Pollution Symposium, vol. 2, Pergamon, Oxford, 1962, pp. 231–266.
[49] F.C. Wu, R.L. Tseng, R.S. Juang, Comparisons of porous and adsorption properties of carbons activated by steam and KOH, J. Colloid Interface Sci. 283 (2005) 49–56.
[50] K. Mohanty, D. Das, M.N. Biswas, Adsorption of phenol from aqueous solutions using activated carbons prepared from *Tectona grandis* sawdust by $ZnCl_2$ activation, Chem. Eng. J. 115 (2005) 121–131.
[51] A. Özer, G. Dursun, Removal of methylene blue from aqueous solution by dehydrated wheat bran carbon, J. Hazard. Mater. 146 (2007) 262–269.
[52] G.E. Boyd, A.W. Adamson, L.S. Meyers, The exchange adsorption of ions from aqueous solution by organic zeolites. II. Kinetics, J. Am. Chem. Soc. 69 (1947) 2836–2848.
[53] D. Reichenberg, Properties of ion exchange resins in relation to their structure. III. Kinetics of exchange, J. Am. Chem. Soc. 75 (1953) 589–597.
[54] A. Mittal, V. Gajbe, J. Mittal, Removal and recovery of hazardous triphenylmethane dye, Methyl Violet through adsorption over granulated waste materials, J. Hazard. Mater. 150 (2008) 364–375.
[55] M.H. Kalavathy, T. Karthikeyan, S. Rajgopal, L.R. Miranda, Kinetic and isotherm studies of Cu(II) adsorption onto H_3PO_4-activated rubber wood sawdust, J. Colloid Interface Sci. 292 (2005) 354–362.
[56] K.V. Kumar, A. Kumaran, Removal of methylene blue by mango seed kernel powder, Biochem. Eng. J. 27 (2005) 83–93.
[57] M. Sathishkumar, A.R. Binupriya, D. Kavitha, S.E. Yun, Kinetic and isothermal studies on liquid-phase adsorption of 2,4-dichlorophenol by palm pith carbon, Bioresour. Technol. 98 (2007) 866–873.
[58] B.H. Hameed, I.A.W. Tan, A.L. Ahmad, Adsorption isotherm, kinetic modeling and mechanism of 2,4,6-trichlorophenol on coconut husk-based activated carbon, Chem. Eng. J. 144 (2008) 235–244.